Characterization, Production and Microwave Absorbing Properties of Polyaniline-$NiFe_2O_4$: Tb Composites

Ethem Ilhan SAHIN [1]*, Selcuk PAKER [2], Mesut KARTAL [2]

[1] *Department of Satellite Communications and Remote Sensing, İstanbul Technical University, Maslak, Istanbul, Turkey*
[2] *Department of Electronics and Communication Engineering, İstanbul Technical University, Maslak, Istanbul, Turkey*

crossref http://dx.doi.org/10.5755/j01.ms.25.3.20810

Received 17 May 2018; accepted 24 July 2018

In this study, terbium-doped $NiFe_2O_4$ was produced by using mixed oxide technique. The $Ni_{1-x}Tb_xFe_2O_4$ composition was synthesized and x was selected as 0.025, 0.050 and 0.070, respectively. The single phase Ni ferrite was produced after sintering at 1250 °C for 4 h. X-ray diffraction (XRD), scanning Electron Microscopy (SEM) and energy-dispersive X-ray spectroscopy (EDS) were performed for the structural analysis. The results of the structural analysis indicated that second phase did not form in $Ni_{1-x}Tb_xFe_2O_4$. Additionally, the polyaniline-terbium doped $NiFe_2O_4$ composites were produced by hot pressing using the compositions of $Ni_{0.975}Tb_{0.025}Fe_2O_{4.018}$, $Ni_{0.950}Tb_{0.050}Fe_2O_{4.037}$, $Ni_{0.93}Tb_{0.070}Fe_2O_{4.0525}$ and aniline. The weight ratios of terbium-doped nickel ferrite and aniline were 1:1 and 1:3 respectively and epoxy resin was used to produce microwave absorbing composites. The magnetic properties of fabricated composites were investigated using a vibrating sample magnetometer (VSM). The microwave absorbing performances of Polyaniline-$NiFe_2O_4$: Terbium composites were investigated by reflectivity in 0 – 8 GHz using two–port vector network analyzer. A minimum of – 39.41 dB reflection performance was obtained in 7.9 GHz at the thickness of 2.0 mm. This reflection performance can be modulated simply by controlling the content of polyaniline in the samples for the required frequency bands.

Keywords: microwave absorber, $NiFe_2O_4$, polyaniline, polymer-matrix composites, reflectivity.

1. INTRODUCTION

Electromagnetic interference has become a threat to information security following the widespread use of wireless communication devices and electronic devices [1]. A way to tackle this problem is to use light and thin high performance electromagnetic wave absorption instruments with a wide absorption range. This absorption material can absorb the electromagnetic waves efficiently and convert the electromagnetic energy into thermal energy or scatter the electromagnetic waves via interference [2].

Electromagnetic wave absorption technology is commonly used in military radars, electromagnetic waves in dark rooms, hidden plating and other technical applications.

MFe_2O_4 (M = Ni, Zn, Cu, Co, etc.) type spinel ferrites are discovered to be significant magnetic materials due to their physiochemical properties [3, 4]. Among these spinel ferrites, $NiFe_2O_4$ is one of the most important soft magnetic ferrites due to its low anti-isotropic wave, chemical stability and low conductance [5, 6]. As an important spinel ferrite, $NiFe_2O_4$ has desirable magnetic properties, high-saturation magnetization, acid resistance and thermal stability, and thus has a high potential for microwave absorbing applications [7, 8].

Even though $NiFe_2O_4$ has good absorption properties, it is also very heavy. In addition, weak electrical conductance and high density of ferrite limits its potential in wide absorption band and electrical conductance applications [9,10].

A method to deal with this problem is mixing or blending pure ferrite dust with non-magnetic polymers [11]. Being light and having good design flexibility, ferrite polymer composites are highly beneficial as microwave absorbers [12 – 14].

In general, conductive polymers are used to prepare microwave absorbing composites [15 – 17]. Among conductive polymers, polyaniline (PANI) is recognized with its unique chemical and physical properties, low cost, good environmental stability and ease of production [18]. Polymer composites are compounds of polymers and organic/inorganic filling materials [19]. Under controlled environments, PANI can be produced by aniline's chemical oxidative polymerization. PANI can also be doped easily and shows sufficient stability [20, 21].

In previous studies In the literature, the microwave absorptive properties of $Ni_{0.6}Zn_{0.4}Fe_2O_4$/PANI composites under a thickness of 2.6 mm were measured using a vector network analyzer at a frequency range of 2 – 18 GHz, and its maximum reflection loss was measured as – 41 dB at 12.8 GHz [22]. In addition, the maximum reflection losses of PANI/ZnO/$CoFe_2O_4$ (CFO) composites were measured as – 41.9 dB at 10.3 GHz with a coating thickness of 3.0 mm [23]. On the other hand, the reflection losses of the prepared PANI/$NiFe_2O_4$/graphite nanosheet composites were measured as – 21 dB at 11.5 GHz with a thickness of 2.0 mm [24].

– 10 dB RL (reflection loss) can be compared with 90% microwave absorption. Therefore, the materials with a RL value less than – 10 dB are considered to be suitable electromagnetic wave absorbers [25].

In this study the single phase $NiFe_2O_4$ ferrites were prepared for the first time by means of mixing oxides by

* Corresponding author. Tel.: +90-212-2853629.
E-mail address: *shnethem@gmail.com* (E.I. Sahin)

adding Tb as solid solution in different ratios instead of Ni in the $NiFe_2O_4$ ferrite composition. New Tb doped $NiFe_2O_4$ and new Tb doped $NiFe_2O_4$: PANI were produced.

2. EXPERIMENTAL SECTION

2.1. Preparation of Tb doped nickel ferrite

Tb doped $NiFe_2O_4$ powder was produced using mixed oxide technique. NiO (Acrosorganic: 99.9 %), Fe_2O_3 (Sigma–Aldrich: 99 %), Tb_4O_7 (Alfa Aesar: 99.9 %) powders were mixed in stoichiometric amounts, according to the $Ni_{1-x}Tb_xFe_2O_4$ compositions in ethanol medium inside a plastic container for 20 h where x = 0.025, 0.050 and 0.070, respectively. After the slurries were dried at 100 °C for 24 h, they were calcined at 600 °C for 4 h in a tightly closed alumina crucible to prevent evaporation losses, which were checked by weighing the samples before and after calcination. After the calcined powders were ground in an agate mortar, they were pressed into pellets with 10 mm diameter and 1 – 2 mm in thickness by using uniaxial press with 2 MPa pressure. The pellets were sintered between the 1200 °C and 1400 °C for 4 h with a heating and cooling rate of 250 °C/h after having buried them in the $NiFe_2O_4$ powder to minimize the loss of volatile species.

The single-phase $NiFe_2O_4$ ferrites were sintered between at 1200 °C – 1300 °C and the Tb-doped $NiFe_2O_4$ reactant powders were sintered at 1250 °C after being calcined at 600 °C.

The phases in the doped sintered samples were characterized by X-ray diffractometry (XRD- D2 Phaser Bruker AXS) with Cu- Kα radiation (λ = 1.5406 Å) in the range 2θ:10 – 70° at a scan rate of 1°/min. The solubility limit, which is defined as the amount that can be doped without disturbing the structure of the main structure ($NiFe_2O_4$), was determined using X-ray powder diffractometry.

The fracture surfaces of the specimens were examined in the scanning electron microscopy SEM (JEOL 5910LV) at 20 kV after being coated with Au/Pd alloy by sputter coater. The chemical analysis was conducted by means of dispersive spectrometry (EDS, Oxford-Inca-7274) and the SEM was used in order to identify the phases and study the microstructure. The magnetic hysteresis measurement (VSM-Cryogenic Limited PPMS) results of the Tb-doped $NiFe_2O_4$ ferrites and the V-doped $NiFe_2O_4$: PANI were determined. The microwave absorber performances of the PANI-$NiFe_2O_4$: Tb composites were measured with the two-port vector network analyzer (R & S FSH-K42) device in the range of 0 – 8 GHz.

2.2. Preparation of polyaniline/$NiFe_2O_4$: Tb composites

The Ni ferrite which has the compositions of $Ni_{0.975}Tb_{0.025}Fe_2O_{4.018}$, $Ni_{0.950}Tb_{0.050}Fe_2O_{4.037}$ and $Ni_{0.93}Tb_{0.070}Fe_2O_{4.0525}$ (account for 100 wt.% and 33 wt.% of aniline quantity), and 1 ml aniline monomer were added in 35 ml hydrochloric acid solution (0.1 mol L^{-1}) and dispersed by mechanical stirring for 30 min. 2.49 g of ammonium persulfate (APS) was dissolved in a 15 ml hydrochloric acid solution (1 mol L^{-1}). The APS solution was then slowly added dropwise to the mixture solution mentioned above by stirring vigorously. Polymerization was carried out in an ice-water bath for 12 h at 0°C. The composites were obtained by filtering and washing the reaction mixture with deionized water, and ethanol, which was then dried under vacuum at 60 °C for 24 h. The PANI/ Ni
ferrite composites with different molar ratios [(Aniline/ $Ni_{0.975}Tb_{0.025}Fe_2O_{4.018}$, Aniline/$Ni_{0.950}Tb_{0.050}Fe_2O_{4.037}$, and Aniline/$Ni_{0.93}Tb_{0.070}Fe_2O_{4.0525}$ = (3:1, 1:1)] were obtained to investigate the influence of the PANI content on the electromagnetic absorption properties. The Tb-doped $NiFe_2O_4$ ferrites were produced as composite with a PANI base. PANI-$NiFe_2O_4$: Tb was produced by hot pressing at different ratios

2.3. Preparation of epoxy-polyaniline/$NiFe_2O_4$: Tb composites

The composite materials were made ready by molding and curing the mixture of PANI/ Tb doped Ni ferrite compositions powders and epoxy. The mixing ratio of the specimen powders to epoxy was 2:1 by weight. Molding was fulfilled in a hydraulic press at 5 MPa pressure and 100 °C for 1 h. They were pressed into pellets with 20 mm diameter and 2 mm thickness for reflectivity measurements. Microwave absorbing composites were manufactured by using epoxy at different ratios of aniline / Tb-added Ni ferrite such as 1/1 and 1/3.

3. RESULTS AND DISCUSSION

3.1. XRD analysis of Tb doped nickel ferrite

The Tb ion was doped into the $NiFe_2O_4$ (PDF Card No: 003-0875) compound to replace the Ni ion since they have close ionic radii values. The doping of Tb into the Nickel ferrite structure was made along the $Ni_{1-x}Tb_xFe_2O_4$ composition with the value of x varying between 0.025 and 0.075. The XRD analysis of the samples sintered at 1250 °C for 4 h revealed that single phase structure was formed for the 0.025, 0.050, 0.070 values of x (Fig. 1).

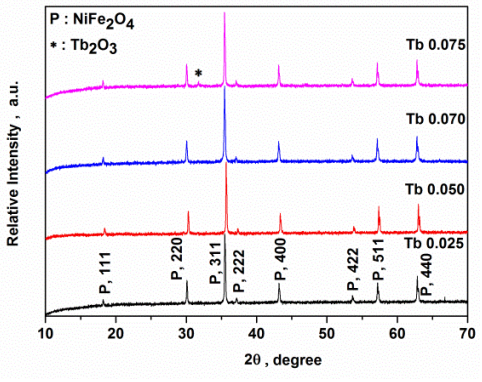

Fig. 1. XRD patterns of Tb doped $Ni_{1-x}Tb_xFe_2O_4$ composition with x = 0.025, 0.050, 0.070 sintered for 4 h at 1250 °C

The single phase formation of the powders was achieved by an appropriate calcination temperature and elimination of the possible intermediate phases by using the mixed oxide synthesis. The well homogenization of the powders enhanced the diffusion process during the heat

treatment. The XRD results indicated that there was no secondary phase in the powders except for 0.075 mol % Tb doped sample. The second phase, that is Tb_2O_3 (PDF Card No: 76-7405), started to appear together with 0.075 mol % Tb doping sample. These results showed that Tb solubility had at limit between x = 0.070 and x = 0.075 in nickel ferrite. Furthermore, $NiFe_2O_4$ formation strongly depends on temperature and high temperatures are required to form single phase $NiFe_2O_4$. The formation temperatures of single phase $NiFe_2O_4$ were also strongly dependent on the type of doping.

3.2. SEM Analysis of Tb Doped Nickel Ferrite

SEM images for the Tb doped Nickel ferrite structure showed that there is only single phase (Fig. 2 a) for x = 0.025.

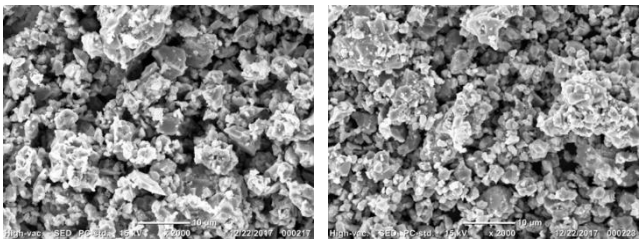

a b

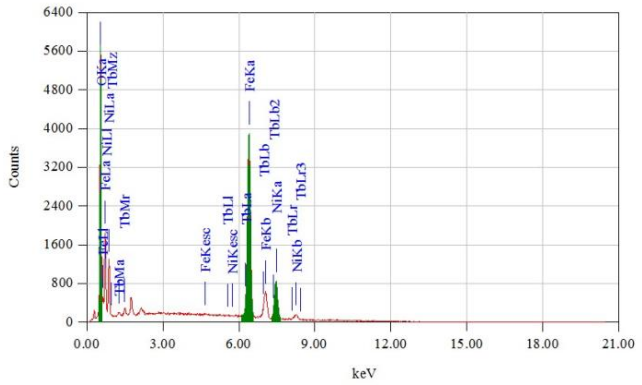

Fe: % 49.12; Ni: % 22.93; O: % 26.38; Tb: % 1.57

c

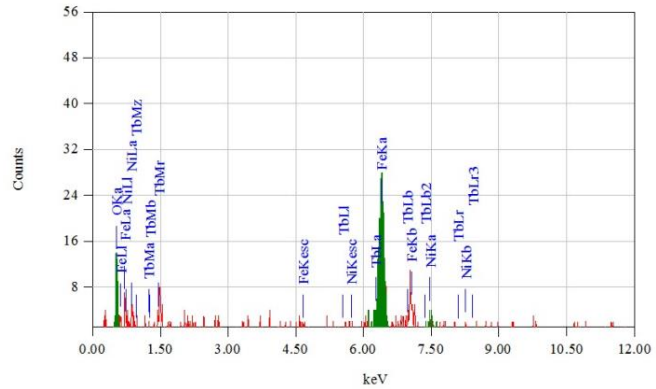

Fe: % 47.59; Ni: % 21.67; O: % 25.81; Tb: % 4.93

d

Fig. 2. SEM images of Tb doped $Ni_{1-x}Tb_xFe_2O_4$ sintered at 1250 °C for 4 h: a – x = 0.025 at × 2.000; b – x = 0.075 at × 2.000; c – EDS analysis of Tb doped $Ni_{1-x}Tb_xFe_2O_4$, x = 0.025 at × 2.000; d – EDS analysis of Tb doped $Ni_{1-x}Tb_xFe_2O_4$, x = 0.075 at × 2.000, the secondary phase (Tb_2O_3) for x = 0.075

However, when the x value was increased to 0.075, a large amount of secondary phase was detected in the structure (Fig. 2 b). While the single phase was determined as Tb containing Nickel ferrite, the other one was Tb_2O_3. The EDS analysis was performed and the images are shown in Fig. 2 c and d). EDS analysis applied to Tb (x = 0.025) doped $NiFe_2O_4$ particles gave similar results to the theoretical composition of Tb doped $NiFe_2O_4$ (% 22.93 Ni, % 49.12 Fe, % 26.38 O, % 1.57 Tb). The content of secondary phase increased with increasing Tb content (Fig. 2 b). By the EDS analysis applied to the secondary phase, it is understood that the ratio of Tb in the structure has increased. By examining from the grain size perspective, it is seen that different Tb dope ratios do not significantly change the Tb doped $NiFe_2O_4$ particle sizes. In addition, the secondary phase formation observed from EDS images was also good agreement with the XRD results.

3.3. Magnetic properties of $NiFe_2O_4$: Tb compositions and PANI/ $NiFe_2O_4$: Tb compositions

Magnetic measurements of Tb_4O_7-doped $NiFe_2O_4$ samples sintered at 1250 °C were performed at room temperature (25 °C) in order to explore the effect of dopants on the magnetic properties. The magnetization of the Tb_4O_7 doped $NiFe_2O_4$ samples at room temperature as a function of magnetic field (M–H) is given in Fig. 3 a.

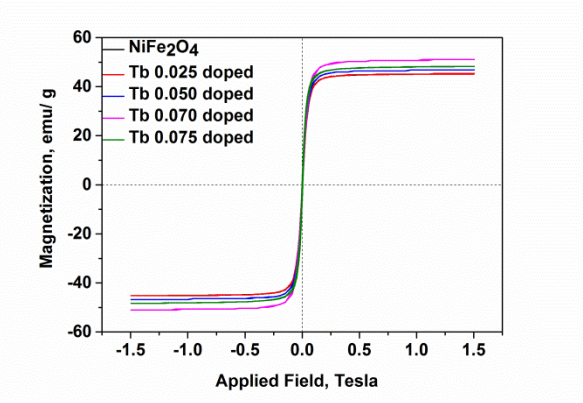

a

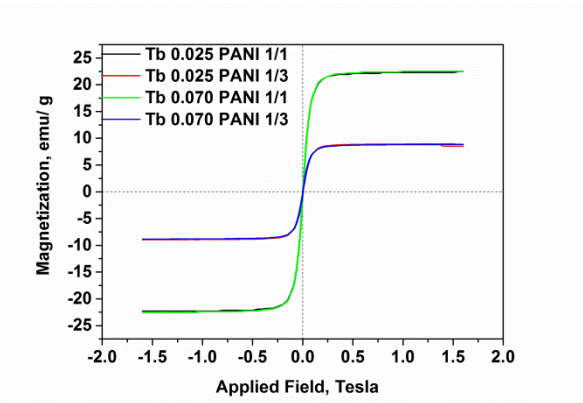

b

Fig. 3. a – magnetic hysteresis loops $NiFe_2O_4$ doped Tb samples (x = 0.025, 0.050, 0.070, 0.075) heat treated at 1250 °C for 4 h; b – magnetic hysteresis loops of $NiFe_2O_4$ doped Tb samples (x = 0.025, 0.070) using PANI (1/3, 1/1) heat treated at 1250 °C for 4 h

A remarkable ferromagnetic behavior was obtained for the $Ni_{1-x}Tb_xFe_2O_4$ sample doped with 0.025 % Tb_4O_7 (x = 0.025), which had saturation magnetization (M_s) of about 45.4 emu/g. As the concentration of the dopant element increased to x = 0.05, the saturation magnetization increased to almost 46.8 emu/g. As the concentration of the dopant element increased to x = 0.07 a further increase to almost 51.1 emu/g was observed in M_s. Thus, it can be concluded that as the Tb dopant element increased, the saturation magnetization also increased.

The magnetization of spinel ferrite can be explained by the Neel's molecular field model. According to this model, the exchange interaction between A-B sites is stronger than A-A and B-B interactions. For x = 0.025, the concentration of Ni $^{+2}$ ions at octahedral B-sites decreases due to the occupation of Tb_4O_7 ions on B-sites. Hence, the change in the magnetic structure results in an increase in saturation magnetization. The increase of $x \geq 0.05$ may be attributed to the distribution of nonmagnetic Tb_4O_7 ions in A and B sites.

When the $Ni_{1-x}Tb_xFe_2O_4$ sample was doped with x = 0.075 Tb_4O_7, a slight decrease down to 48.3 emu/g was noted in M_s. As the PANI concentration decreased from 1:1 to 1:3, saturation magnetization also decreased as expected.

The magnetic field dependent magnetization at 1250 °C for the Tb_4O_7 doped $Ni_{1-x}Tb_xFe_2O_4$ samples (x = 0.025) with different PANI concentrations (1/3 and 1/1) is shown in Fig. 3 b. Both samples showed different ferromagnetic behavior. While The Ms for the sample with a PANI concentration of 1/3 appeared less with a value of approximately 8.96 emu/g, the sample with a PANI concentration of 1/1 showed higher M_s with a value of approximately 22.5 emu/g. Similarly, the Tb_4O_7 doped $Ni_{1-x}Tb_xFe_2O_4$ samples (x = 0.070) with different PANI concentrations (1/3 and 1/1) showed ferromagnetic behavior with M_s = 8.85 and 22.5 emu/g respectively.

3.4. Reflectivity measurements of Tb doped nickel ferrite

Fig. 4 shows the frequency dependence of the reflection loss of the Epoxy-PANI/$NiFe_2O_4$: Tb composites in the frequency range of 0 – 8 GHz. Among the PANI-$NiFe_2O_4$: Tb composites, it can be seen that epoxy-$NiFe_2O_4$: Tb composites/Aniline:1/3 had a more observable effect on microwave absorption properties than epoxy-$NiFe_2O_4$: Tb composites/Aniline:1/1. The PANI/Tb doped Ni ferrite compositions ($Ni_{0.975}Tb_{0.025}Fe_2O_{4.018}$/Aniline:1/1) powders and epoxy showed only one band with – 23.06 dB at 7.55 GHz and this composite material achieved a reflection less than – 10 dB in the frequency band between 5.66 GHz and 6.70 GHz. When the nickel ferrite powder content decreased, the epoxy-PANI/ Tb doped Ni ferrite compositions ($Ni_{0.975}Tb_{0.025}Fe_2O_{4.018}$/Aniline:1/3) reached to – 29.2 dB at 7.187 GHz in reflection loss (Fig. 4 a) and this composite material achieved a reflection less than – 20 dB in the frequency band between 5.37 GHz and 6.55 GHz, moreover, it achieved a reflection less than – 10 dB in the frequency bands between 3.30 and 6.72 GHz, 6.85 GHz and 8 GHz.

The epoxy-PANI/Tb doped Ni ferrite compositions ($Ni_{0.950}Tb_{0.050}Fe_2O_{4.037}$/Aniline:1/3) reached to – 37.205 dB at 7.56 GHz in reflection loss (Fig. 4 b). In addition, the best overall reflection loss performance was achieved with this composition, which shows a value less than – 20 dB in the frequency bands between 5.12 GHz and 6.68 GHz, 6.90 GHz and 8 GHz. Moreover, it achieved a reflection less than – 10 dB in the frequency band between 1.24 GHz and 6.71 GHz in reflection loss (Fig. 4 b).

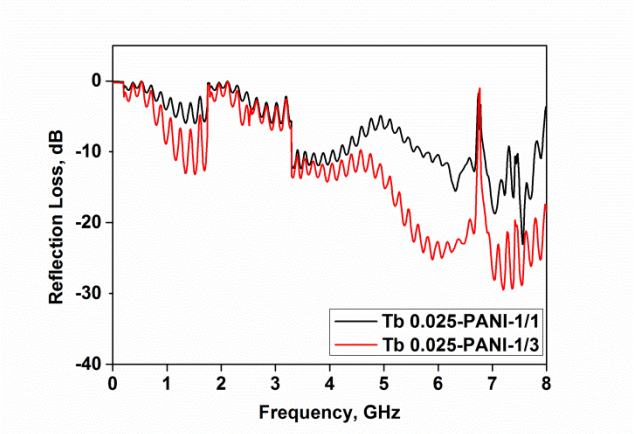

a

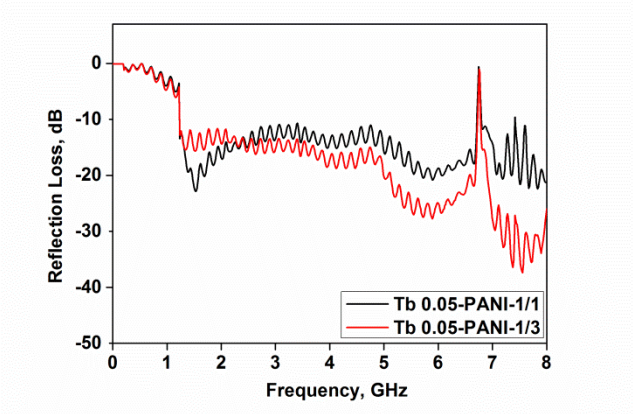

b

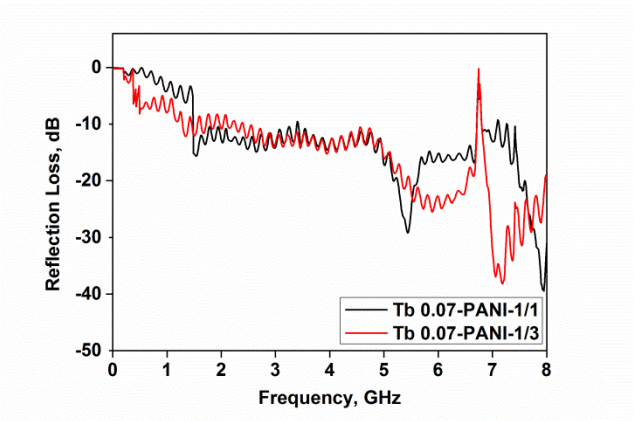

c

Fig. 4. Microwave absorption properties of the epoxy-PANI-$NiFe_2O_4$: Tb composites: a – x = 0.025, Tb-added Ni ferrite/Aniline compositions of $Ni_{0.975}Tb_{0.025}Fe_2O_{4.018}$ weight ratio was changed as 1:1, 1:3; b – x = 0.050, Tb-added Ni ferrite/Aniline compositions of $Ni_{0.950}Tb_{0.050}Fe_2O_{4.037}$ weight ratio was changed as 1:1, 1:3; c – x = 0.070, Tb-added Ni ferrite/Aniline compositions of $Ni_{0.93}Tb_{0.070}Fe_2O_{4.0525}$ weight ratio was changed as 1:1, 1:3

The PANI/Tb doped Ni ferrite composition ($Ni_{0.950}Tb_{0.050}Fe_2O_{4.037}$/Aniline:1/1) powders and epoxy showed only one band with – 22.25 dB at 7.83 GHz and this composite material achieved a reflection less than – 10 dB in the frequency band between 1.246 GHz and 6.71 GHz.

The PANI/Tb doped Ni ferrite composition ($Ni_{0.93}Tb_{0.070}Fe_2O_{4.0525}$/Aniline:1/1) powders and epoxy showed only two bands with – 39.51 dB and – 29.21 dB at 7.95 GHz and 5.44 GHz and this composite material achieved a reflection less than – 20 dB in the frequency band between 7.48 GHz and 8 GHz. Moreover, it achieved a reflection less than – 10 dB in the frequency bands between 3.42 GHz and 6.72 GHz, 1.47 GHz and 3.389 GHz.

The other second best overall reflection loss performance was achieved with the $Ni_{0.93}Tb_{0.070}Fe_2O_{4.0525}$/Aniline:1/3 composition (Fig. 4 c) which showed a value less than – 20 dB in the frequency bands between 5.31 GHz and 6.53 GHz, 6.91 GHz and 8 GHz, this composite material achieved a reflection less than – 10 dB in the frequency band between 2.42 GHz and 6.69 GHz. Moreover, this composition ($Ni_{0.93}Tb_{0.070}Fe_2O_{4.0525}$/Aniline:1/3) reached to – 37.98 dB at 7.18 GHz in reflection loss (Fig. 4 c). In Fig. 4 part, when Tb (x = 0.070), the solubility increased when Tb element settles into $NiFe_2O_4$, structured its environment according to itself, increased the wave interference by the increasing surface area and increased the absorption. As PANI content increases, and powder amount decreases, the absorption increased. Matching of impedance has been achieved by using PANI. PANI effect has increased the absorption.

Besides, interfacial polarization between PANI and Tb doped $NiFe_2O_4$ plays an important role in the electromagnetic absorbing material. The performance of microwave absorber also depends on the matching of the impedance of the irradiation on the surface of the material. PANI improves the matching impedance on the transmissions between the ingredients of the composites.

It is observed that the EM absorber property is due to actually the magnetic spinel ferrite Ni. Meantime, the sharp absorption peaks appear owing to the influence of conductive polymer PANI. Conducting Polymer PANI has been used in especial to reduce the influence of existing eddy currents, since the permeability of magnetic materials at high frequencies will decrease Eddy currents generated by EM waves. PANI creates electrical loss. It was mixed with spinel magnetic materials such as Ni and with the magnetic absorption feature provide to control EM absorptivity. In reality, the changes such as the magnetocrystalline anisotropy, saturation magnetization, dielectric properties and resonance frequency shifting of the material were provided. So, the effect of this is apparent in the material, and the absorption peak is shifted to the high frequency region.

4. CONCLUSIONS

Tb doped $NiFe_2O_4$ was produced along with $Ni_{1-x}Tb_xFe_2O_4$ compositions by using mixed oxide technique and PANI-$NiFe_2O_4$:Tb composites were produced for the first time in literature, to our knowledge. The Tb solubility in $NiFe_2O_4$ was much higher (x = 0.070). The secondary phase could be identified as Tb_2O_3 in Tb doping.

SEM investigation also confirmed the XRD results, as Tb doping gave only single phase at x = 0.070 and below. The minimum reflection point shifted towards higher frequency with an increase of PANI content for epoxy - PANI/ $NiFe_2O_4$:Tb compositions. Among epoxy-PANI/ $NiFe_2O_4$:Tb compositions, the $Ni_{0.950}Tb_{0.050}Fe_2O_{4.037}$/Aniline:1/3 and the $Ni_{0.93}Tb_{0.070}Fe_2O_{4.0525}$/Aniline:1/3 gave the best overall reflection performance in the frequency bands.

The magnetic value in the highest Tb doped $NiFe_2O_4$ structure gave better results.

The microwave absorption property was obtained at 7.95 GHz and 2.0 mm in thickness with the minimum RL of – 39.51 dB by $Ni_{0.93}Tb_{0.070}Fe_2O_{4.0525}$/Aniline:1/1 composite. Microwave absorbing properties can be modulated simply by controlling the content of PANI and the effect of Tb dopant on the samples for the required frequency bands. Due to the easy and low cost preparation methods and reflectivity performance, the PANI/Tb doped nickel ferrite composites have a promising potential as microwave absorbers. The dopants and PANI were used to improve the microwave absorber properties of $NiFe_2O_4$. Microwave absorbing properties of Tb doped $NiFe_2O_4$ PANI compositions show a consistent variation with high Tb doping amounts. The best reflection loss performance was obtained from $Ni_{0.950}Tb_{0.050}Fe_2O_{4.037}$/Aniline:1/3 composition at the value of less than – 20 dB and between 5.12 GHz and 6.68 GHz, 6.90 GHz and 8 GHz. The content of PANI plays an important role in the variation of absorbing properties. The microwave absorbing properties of the Tb doped $NiFe_2O_4$: PANI compositions can be investigated for a broader concentration range of Tb dopant below 0.075 than those used in this study. Tb doped $NiFe_2O_4$: PANI can be considered as a candidate for microwave absorbers in a broadwidth range. Dopant formation is another area of interest regarding nickel ferrite. Dopants and PANI content have been used to improve the microwave absorbing properties of $NiFe_2O_4$. The microwave absorption properties of PANI-single phase Tb doped $NiFe_2O_4$ at high frequencies may also be determined.

Acknowledgment

This study was supported by the Scientific Research Office (BAP) of İstanbul Technical University (Project Number: 39309). This study is attributed to Prof. Dr. Ayhan Mergen who passed away in August, 2017. The authors would like to express their gratitude to him for his friendship, comments and faithful collaboration.

REFERENCES

1. **Sun, C., Guo, Y., Xu, X., Du, Q., Duan, H., Chen, Y., Li, H., Liu, H.** In Situ Preparation of Carbon/Fe_3C Composite Nanofibers with Excellent Electromagnetic Wave Absorption Properties *Composites: Part A* 92 2017: pp. 33 – 41. https://doi.org/10.1016/j.compositesa.2016.10.033
2. **Li, Z., Ye, M., Han, A., Du, H.** Preparation, Characterization and Microwave Absorption Properties of $NiFe_2O_4$ and Its

Composites with Conductive Polymer *Journal of Materials Science: Materials in Electronics* 27 2016: pp. 1031 – 1043. https://doi.org/10.1007/s10854-015-3848-8

3. **Cao, D., Pan, L., Li, H., Li, J., Wang, X., Cheng, X., Wang, Z., Wang, J., Liu, Q.** A facile Strategy for Synthesis of Spinel Ferrite Nano-Granules and Their Potential Applications *RSC Advances* 6 2016: pp. 66795 – 66802. https://doi.org/10.1039/c6ra13373h
4. **Zhu, Z., Liu, F., Zhang, H., Zhang, J., Han, H.** Photocatalytic Degradation of 4-Chlorophenol Over Ag/MFe_2O_4 (M = Co, Zn, Cu, and Ni) Prepared by A Modified Chemical Co-Precipitation Method: A Comparative Study *RSC Advances* 5 2015: pp. 55499 – 55512. https://doi.org/10.1039/c5ra04608d
5. **Kavas, H., Kasapoğlu, N., Baykal, A., Köseoğlu, Y.** Characterization of $NiFe_2O_4$ Nanoparticles Synthesized by Various Methods *Chemical Papers* 63 (4) 2009: pp. 450 – 455. https://doi.org/10.2478/s11696-009-0034-6
6. **Zhang, Z., Liu, Y., Yao, G., Zu, G., Hao, Y.** Synthesis and Characterization of $NiFe_2O_4$ Nanoparticles Via Solid-State Reaction *International Journal of Applied Ceramic Technology* 10 (1) 2013: pp. 142 – 149. https://doi.org/10.1111/j.1744-7402.2011.02719.x
7. **Cheng, B., Chen, X., Wang, X., Qiu, H., Qi, S.** Preparation and Microwave Absorbing Performance of TiO_2/$NiFe_2O_4$/Hollow Glass Microsphere Composite with Core-Shell Structure *Journal of Materials Science: Materials in Electronics 28* 2017: pp. 7575 – 7581. https://doi.org/10.1007/s10854-017-6449-x
8. **Chen, X., Huang, Y., Zhang, K., Feng, X., Li, S.** Self-Assembled Flower-Like $NiFe_2O_4$ Decorated on 2D Graphene Nanosheets Composite and Their Excellent Electrochemical Performance as Anode Materials for LIBs *Journal of Alloys and Compounds* 686 2016: pp. 905 – 913. https://doi.org/10.1016/j.jallcom.2016.06.244
9. **Choi, M.K., Park, I., Kim, D.C., Joh, E., Park, O.K., Kim, J., Kim, M., Choi, C., Yang, J., Kyoung, W.C.** Thermally Controlled, Patterned Graphene Transfer Printing for Transparent and Wearable Electronic/Optoelectronic System *Advanced Functional Mater*ials 25 2015: pp. 7109 – 7118. https://doi.org/10.1002/adfm.201502956
10. **Xu, J., Wang, K., Zu, S.Z., Han, B.H., Wei, Z.** Hierarchical Nanocomposites of Polyaniline Nanowire Arrays on Graphene Oxide Sheets with Synergistic Effect for Energy Storage *ACS Nano* 4 (9) 2010: pp. 5019 – 502. https://doi.org/10.1021/nn1006539
11. **Tsutaoka, T.** Frequency Dispersion of Complex Permeability in Mn–Zn and Ni–Zn Spinel Ferrites and Their Composite Materials *Journal of Applied Physics* 93 2003: pp. 2789 – 2796. https://doi.org/10.1063/1.1542651
12. **Pardavi Horvath, M.** Microwave Applications of Soft Ferrites *Journal of Magnetism and Magnetic Materials* 215 – 216 2000: pp. 171 – 183. https://doi.org/10.1016/S0304-8853(00)00106-2
13. **Verma, A., Saxena, A.K., Dube, D.C.** Microwave Permittivity and Permeability of Ferrite–Polymer Thick Films *Journal of Magnetism and Magnetic Materials* 263 2003: pp. 228 – 234. https://doi.org/10.1016/S0304-8853(02)01569-X
14. **Cho, S.B., Kang, D.H., Oh, J.H.** Relationship Between Magnetic Properties and Microwave-Absorbing Characteristics of NiZnCo Ferrite Composites *Journal of Materials Science* 31 1996: pp. 4719 – 4722. https://doi.org/10.1007/BF00366375
15. **Yang, J., Zhou, Y., Sun, L., Zhao, N., Zang, C., Cheng, X.** Synthesis, Characterization and Optical Property of Graphene Oxide Films *Applied Surface Science* 258 2012: pp. 5056 – 5060. https://doi.org/10.1016/j.apsusc.2012.01.105
16. **Yuchang, Q., Dandan, M., Yingying, Z., Fa, L., Wancheng, Z.** Graphene Nanosheet- and Flake Carbonyl Iron Particle-Filled Epoxy–Silicone Composites as Thin–Thickness and Wide-Bandwidth Microwave Absorber *Carbon* 86 2015: pp. 98 – 107. https://doi.org/10.1016/j.carbon.2015.01.002
17. **Jiang, J., Li, L., Xu, F.** Polyaniline–LiNi Ferrite Core–Shell Composite:Preparation, Characterization and Properties *Materials Science and Engineering A* 456 2007: pp. 300 – 304. https://doi.org/10.1016/j.msea.2006.11.143
18. **Yang, C.C., Gung, Y.J., Hung, H., Ting, T.H., Wu, K.H.** Infrared and Microwave Absorbing Properties of $BaTiO_3$/ Polyaniline and $BaFe_{12}O_{19}$/ Polyaniline Composites *Composites Science and Technology* 70 2010: pp. 466 – 471. https://doi.org/10.1016/j.compscitech.2009.11.021
19. **Ansari, M.A., Mohammad, F.** Thermal Stability, Electrical Conductivity and Ammonia Sensing Studies on p-Toluenesulfonic Acid Doped Polyaniline:Titanium Dioxide (pTSA/Pani:TiO_2) Nanocomposites *Sensors and Actuators B* 157 2011: pp. 122 – 129. https://doi.org/10.1016/j.snb.2011.03.036
20. **Schnitzler, D.C., Meruvia, M.S., Hümmelgen, I., Aldo, J., Zarbin, G.** Preparation and Characterization of Novel Hybrid Materials Formed from (Ti,Sn)O_2 Nanoparticles and Polyaniline *Chemistry of Materials* 15 (24) 2003: pp. 4658 – 4665. https://doi.org/10.1021/cm034292p
21. **Ma, X., Zhang, X., Li, Y., Li, G., Wang, M., Chen, H., Mi, Y.** Preparation of Nano-Structured Polyaniline Composite Film Via ''Carbon Nanotubes Seeding'' Approach and its Gas-Response Studies *Macromolecular Materials and Engineering* 1 (291) 2006: pp. 75 – 82. https://doi.org/10.1002/mame.200500296
22. **Wang, M., Guangbin, J., Zhang, B., Tang, D., Yang, Y., Du, Y.** Controlled Synthesis and Microwave Absorption Properties of $Ni_{0.6}Zn_{0.4}Fe_2O_4$/PANI Composite Via an in-Situ Polymerization Process *Journal of Magnetism and Magnetic Materials* 377 2015: pp. 52 – 58. https://doi.org/10.1016/j.jmmm.2014.10.066
23. **Lin, Y., Wang, J., Yang, H., Wang, L.** In Situ Preparation of PANI/ZnO/$CoFe_2O_4$ Composite with Enhanced Microwave Absorption Performance *Journal of Materials Science: Materials in Electronics* 28 2017: pp. 17968 – 17975. https://doi.org/10.1007/s10854-017-7739-z
24. **Chen, X., Qi, S.** Preparation and Microwave Absorbing Properties of Polyaniline/$NiFe_2O_4$/Graphite Nanosheet Composites Via Sol–Gel Reaction and in Situ Polymerization *Journal of Sol-Gel Science and Technology* 81 2017: pp. 824 – 830. https://doi.org/10.1007/s10971-016-4226-6
25. **Wang, G.Z., Gao, Z., Wan, G.P., Lin, S.W., Yang, P., Qin, Y.** High Densities of Magnetic Nanoparticles Supported on Graphene Fabricated by Atomic Layer Deposition and Their Use as Efficient Synergistic Microwave Absorbers *Nano Research* 7 2014: pp. 704 – 716. https://doi.org/10.1007/s12274-014-0432-0